**Mater. Res. Soc. Symp. Proc. Vol. 924 © 2006 Materials Research Society** **0924-Z08-31**

# ELASTODYNAMIC CHARACTERIZATION OF IMPRINTED NANOLINES

Ward L. Johnson[1], Colm M. Flannery[1], Sudook A, Kim[1], Roy Geiss[1], Paul R. Heyliger[2], Chris L. Soles[3], Walter Hu[4], and Stella W. Pang[4]

[1]Materials Reliability Division, National Institute of Standards and Technology, Boulder, CO, 80305

[2]Department of Civil Engineering, Colorado State University, Fort Collins, CO, 80523

[3]Polymers Division, National Institute of Standards and Technology, Gaithersburg, MD, 20899

[4]Department of Electrical Engineering and Computer Science, University of Michigan, Ann Arbor, MI, 48109

## ABSTRACT

The advancement of imprint lithography as a method for fabricating nanostructures is impeded by a lack of effective tools for characterizing mechanical properties and geometry at the nanoscale. This paper describes progress in establishing methods for determining elastic moduli and cross sectional dimensions of imprinted nanolines from Brillouin light scattering (BLS) measurements using finite-element (FE) and Farnell-Adler models for the vibrational modes. An array of parallel nanoimprinted lines of polymethyl methacrylate (PMMA) with widths of ~65 nm and heights of ~140 nm served as a model specimen. Several acoustic modes were observed with BLS in the low-gigahertz frequency range, and the forms of the vibrational displacements were identified through correlation with calculations using measured bulk-PMMA moduli and density as input. The acoustic modes include several flexural, Rayleigh-like, and Sezawa-like modes. Fitting of Farnell-Adler calculations to the measured dispersion curves was explored as a means of extracting elastic moduli and nanoline dimensions from the data. Some of the values obtained from this inversion analysis were unrealistic, which suggests that geometric approximations in the model introduce significant systematic errors. In forward calculations, the frequencies determined with the FE method were found to more closely match experimental values, which suggests that this method may be more accurate for inversion analysis. Initial estimates of uncertainties in the FE calculations support this conclusion.

## INTRODUCTION

Nanoimprint lithography (NIL) has emerged as a leading candidate for relatively low-cost nanoscale patterning of materials. It has attracted particular attention as a method for fabricating patterned polymers with length scales beyond the fundamental limits of conventional photolithography used for integrated circuits. However, numerous technical obstacles must be overcome before NIL reaches the point of broad industrial implementation [1]. These obstacles primarily are associated with the mechanical behavior of imprinted material during stamping, cooling, and removal from the mold. To successfully model and optimize these processes, one must have information on the mechanical properties of the material, which generally is unattainable from conventional techniques because of the length scales involved. Direct measurements of the elastic moduli of imprinted polymeric nanostructures are especially important because of the expected deviations from bulk values and appearance of elastic anisotropy when dimensions approach the scale of the macromolecular diameters (typically, tens of nanometers) [2].

In collaboration with the University of Akron, we previously explored the use of Brillouin light scattering (BLS) for characterizing the vibrational modes and elastic moduli of nanolines [3]. The specimens in that study were photolithographically patterned arrays of nanolines of photoresist fabricated on oxidized silicon with an antireflective coating. The symmetries of the three lowest-frequency modes of these nanolines were determined through comparisons of data with calculations using FE methods and the general method of Farnell and Adler [4]. The lowest mode was found to be flexural (with displacements primarily parallel to the substrate and perpendicular to the long axis of the nanolines). The second and third modes were found to be similar to the Rayleigh and lowest Sezawa modes of a blanket film.

Proceeding from the work of Ref. 3, we present, in this report, measurements and modeling of imprinted nanolines of a well characterized polymer on a bare substrate. FE and Farnell-Adler models are modified to enhance the accuracy and/or speed of calculations, an inversion algorithm is implemented for extracting elastic moduli and line dimensions using the Farnell-Adler method, and the accuracy of this inverse calculation is assessed.

## MEASUREMENTS

A model specimen was fabricated by imprinting an array of parallel polymethyl methacrylate (PMMA) nanolines onto (100) silicon. The length of the nanolines was 10 $\mu$m. A residual PMMA layer between the nanolines was present after imprinting, and this was removed by a plasma etch. Figure 1 shows an image of a section of the array obtained using field-emission scanning electron microscopy (FESEM) with a beam energy of 500 V, which is low enough to avoid evaporation of the PMMA. From critical-dimension small-angle x-ray scattering (CD-SAXS) measurements, the cross sections of the nanolines after etching were determined to have a height $h$ (dimension perpendicular to the substrate) of 140 nm, a width $w$ of 65 nm, and a periodicity of 359 nm. The CD-SAXS data also indicated that there was significant deviation from rectangular geometry, but the detailed shape was not determined.

BLS measurements were performed in a backscattering configuration with the incident laser beam, axis of the collection lens, and long axis of the nanolines in a common plane. The measurements were performed at a series of angles $\theta$ between the incident beam and the normal of the substrate, providing selective detection of acoustic wavelengths along the nanolines in the range of 270 nm to 464 nm. Inelastically scattered light was passed without polarization filtering to a standard scanning (3+3)-pass tandem Fabry-Perot interferometer.

A representative BLS spectrum with $\theta$ equal to 70° is shown in Fig. 2. The incident angle corresponds to a wave number $k$ (2π/wavelength) of 22.2 $\mu m^{-1}$ for the detected acoustic modes, through the relation $k = (4\pi/\lambda_0)\cdot\sin\theta$, where $\lambda_0$ is the laser wavelength, 532 nm. The large central peak, which arises from light that is reflected from the specimen with no change in frequency, obscures a peak near 2.7 GHz that is more clearly seen when the spectrometer is configured to scan over a smaller range of frequencies. The frequency shifts of the peaks were determined by fitting to Lorentzian functions. The two highest-frequency peaks were assumed each to be

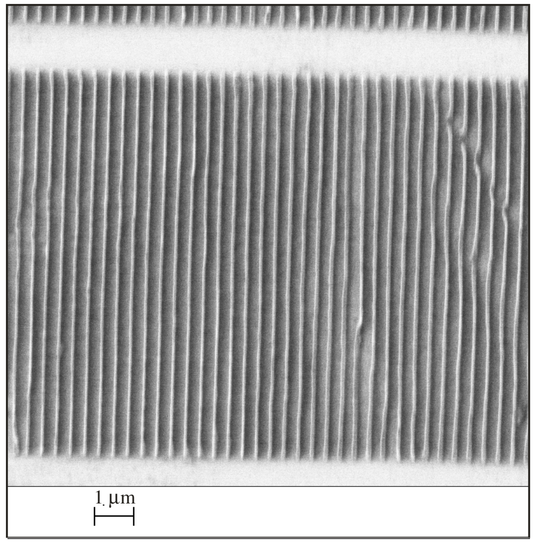


**Figure 1**. SEM image of a section of the array of PMMA nanolines.

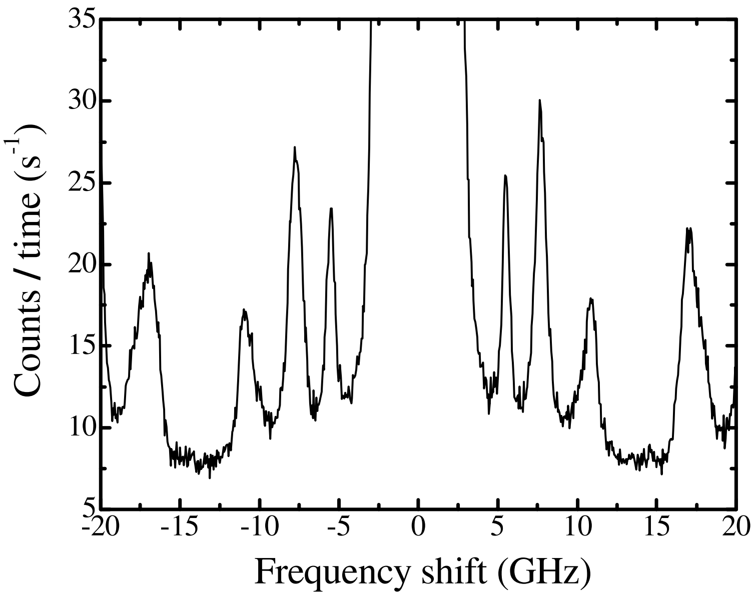


**Figure 2**. BLS spectrum with an angle of 70º between the substrate normal and the incident beam. Ordinates are the counts per unit time in one channel of the multichannel analyzer.

superpositions of two closely spaced peaks (because of their asymmetrical shape) and were fit to a sum of two Lorentzians. Dispersion curves obtained in this manner are shown in Fig. 3.

To provide input parameters for numerical modeling of acoustic modes, BLS measurements of bulk longitudinal and shear waves were performed on a plate of PMMA with a thickness of approximately 17 $\mu$m. The starting material for this plate was the same as that for the imprinted PMMA nanolines. From the BLS measurements, the longitudinal velocity $v_1$ and shear velocities $v_2$ were determined to be 2784 m/s and 1354 m/s, respectively, assuming the

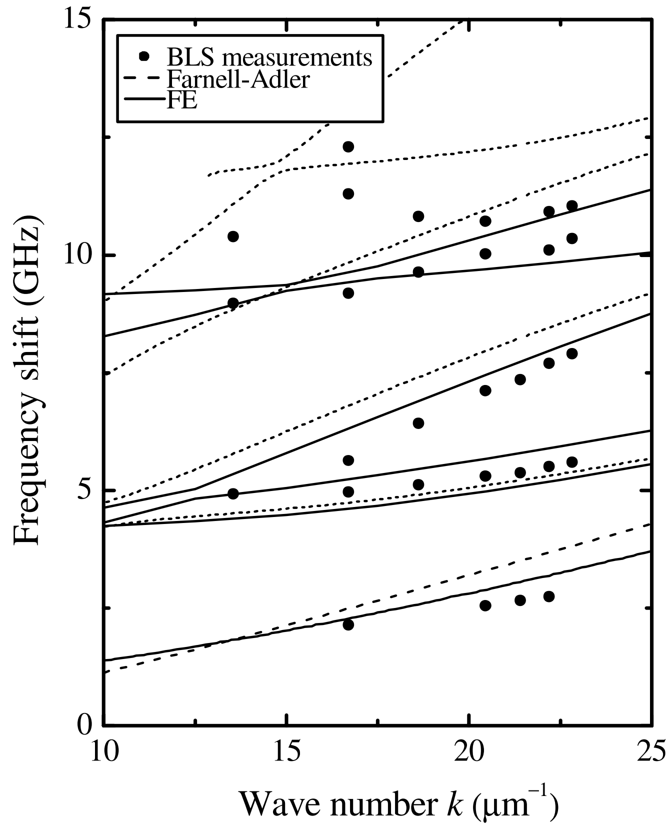


**Figure 3**. BLS measurements. Farnell-Adler calculations and FE calculations with $v_1$ = 2784 m/s, $v_2$ = 1354 m/s, $\rho$ = 1187 kg/m$^3$, $h$ = 140 nm, and $w$ = 65 nm.

index of refraction is 1.49 [5]. The density $\rho$ of a larger piece of PMMA (from different starting material) was determined to be 1187 kg/m$^3$ by Archimedes' method. These measured values for the velocities and density correspond to elastic moduli $C_{11}$ = 9.20 GPa and $C_{44}$ = 2.18 GPa.

## ANALYSIS AND DISCUSSION

FE calculations of the six lowest-frequency modes were performed with the QR algorithm (a standard eigensolver) using the elastic moduli and density measured on bulk PMMA (above) and the approximation of a rectangular cross section with $h$ = 140 nm and $w$ = 65 nm (as estimated from CD-SAXS analysis). These calculations were confined to the PMMA, with the PMMA/silicon interface approximated as completely rigid. Initially, a three-dimensional mesh extending over the full 10 $\mu$m length of the nanoline was employed. However, computation times were found to be impractical when mesh spacings were reduced towards the size necessary to achieve sufficient accuracy (as reflected in convergence of the calculated frequencies). Therefore, the calculations were simplified by assuming sinusoidal variation of the displacements along the length of the nanoline (eliminating the need for a FE mesh along the length). Figure 3 shows FE calculations of this type with a mesh of 16 x 32 points over the cross section. Corresponding displacement patterns (not shown) show that the lowest and second-lowest modes are flexural and Rayleigh-like, respectively, with forms similar to those that we presented in Ref. 3. The third mode is a higher-order flexural mode, with greater vertical phase variation. The fourth, fifth, and sixth modes are the lowest Sezawa-like, third flexural, and second Sezawa-like modes, respectively.

Through comparison with the FE calculations, the lowest-frequency measured dispersion curve in Fig. 3 is unambiguously identified with the lowest flexural mode. The identification of the second-lowest experimental dispersion curve is less straightforward, since it lies between the FE calculations of the Rayleigh-like and second flexural modes. Two factors suggest that this curve arises from the Rayleigh-like mode and that the second flexural mode is not detected in BLS: 1) the symmetry of displacements of Rayleigh modes typically leads to relatively strong BLS peaks, and 2) the second peak does not show, at any measured wave number, evidence for it being a superposition of two peaks. The third measured dispersion curve clearly arises from the lowest Sezawa-like mode.

The frequency of the lowest flexural mode previously was determined through Farnell-Adler calculations to be approximated by that of the lowest-frequency antisymmetric Lamb (flexural) mode of an infinite plate with thickness $w$ [3]. However, the closer correspondence of FE calculations to the measured frequencies in Ref. 3 suggests that significant inaccuracy in the Farnell-Adler calculations was introduced by the approximation of infinite nanoline height. To make the Farnell-Adler calculations of this flexural mode more accurate, we have approximated the effect of finite height using the transverse-resonance approach of Lagasse *et al*. [6,7]. These calculations are shown in Fig. 3 (lowest dashed curve) with $h$ = 140 nm, $w$ = 65 nm, measured bulk velocities of the PMMA plate, and measured $\rho$ of bulk PMMA. Although the transverse-wave approach brings the Farnell-Adler results closer to the FE results, significant discrepancy remains at the higher wave numbers.

The second and third measured dispersion curves in Ref. 3 were approximated by Rayleigh and Sezawa waves of a blanket film on silicon, with the thickness of the film taken to be the nanoline height plus the antireflective-coating thickness. In Fig. 3, the higher-frequency dashed curves are similar Farnell-Adler calculations. However, since there is no complicating intermediate layer, the film thickness in these calculations is simply $h$ (140 nm). The input parameters also include published values for the density and elastic moduli of silicon [8]. The wave vectors were along the <011> direction of silicon.

Inversion analyses of the BLS data were attempted using the Farnell-Adler method with the nanoline cross-sectional dimensions and elastic moduli as adjustable parameters. A Monte-Carlo technique first was used to locate the region of the global minimum of the difference between the calculations and the data, and, then, a quasi-Newton minimization algorithm was used to refine this. The parameters determined from a fit to the lowest two dispersion curves (flexural and Rayleigh-like) were $v_1$ = 2347 m/s, $v_2$ = 1332 m/s, $h$ = 120 nm, and $w$ = 52 nm; and those determined from a fit to the lowest three curves (including the lowest Sezawa-like mode) were $v_1$ = 2154 m/s, $v_2$ = 1223 m/s, $h$ = 106 nm, and $w$ = 54 nm. These values for $h$ are much different from that determined from CD-SAXS analysis, and those for $v_1$ are much different from that expected from BLS measurements on bulk PMMA. The elastic moduli are not expected to differ significantly from bulk values when dimensions are in the range of this specimen [2]. The fact that the forward FE calculations in Fig. 3 more closely match the BLS data suggests that significant inaccuracy remains from neglecting the finite cross sectional dimensions in the

Farnell-Adler calculations (for the Rayleigh-like and Sezawa-like modes) and that this is the reason for unrealistically low values obtained from the inversion analysis.

To explore the potential of the FE method for more accurate inversion analysis, systematic errors introduced by the sinusoidal and fixed-interface approximations in the FE calculations were estimated using FE calculations with and without sinusoidal approximations and Farnell-Adler calculations with and without rigid interfaces. These suggest that systematic errors are not significant for the lowest three modes when wave numbers are above ~15 $\mu m^{-1}$. A complete description of these analyses will be presented elsewhere, along with results of inverse FE calculations.

## CONCLUSION

This report describes progress towards the goal of establishing methods for the determination of elastic moduli and geometry of imprinted nanolines from BLS measurements. It goes beyond the previously published work of Hartschuh *et al.* [3] by 1) considering imprinted nanolines on a bare substrate (rather than lithographically patterned photoresist with an antireflective coating), 2) incorporating estimates of the effect of finite cross sectional geometry in Farnell-Adler calculations of the flexural mode, 3) including elastic anisotropy of a single-crystal substrate in the Farnell-Adler calculations, 4) increasing the accuracy and speed of FE calculations, 5) using measured bulk material parameters in the forward calculations, and 6) performing initial inversion analysis using Farnell-Adler models. Some of the values obtained for moduli and dimensions in the inverse Farnell-Adler calculation are significantly lower than expected, and this is attributed to inaccuracy of the approximation of a blanket film in the models for the Rayleigh-like and Sezawa-like modes. The FE method is now well positioned for implementation in a more accurate inversion algorithm, with greatly increased speed and evidence for the validity of approximations that are incorporated in the model.



## REFERENCES


1. L.J. Guo, J. Phys. D: Appl. Phys. **37,** R123 (2004).
2. K. Van Workum and J.J. de Pablo, Nano Lett., **3** 1405 (2003).
3. R.D. Hartschuh, A. Kisliuk, V. Novikov, A.P. Sokolov, P.R. Heyliger, C.M. Flannery, W.L. Johnson, C.L. Soles, and W.-L. Wu, Appl. Phys. Lett., **87**, 173121 (2005).
4. G. Farnell and E. Adler, in *Physical Acoustics, Vol. 9*, ed. by W. P. Mason and N. Thurston, (Academic Press, New York, 1972), pp. 35-87.
5. K. Gieck and R. Gieck, *Engineering Formulas* (McGraw-Hill, New York, 1997).
6. P.E. Lagasse, I.M. Mason and E.A. Ash, IEEE Trans. Microwave Theory Tech., **21**, 225, (1973).
7. P.E. Lagasse, I.M. Mason and E.A. Ash, IEEE Trans. Sonics Ultrason., **20**, 143 (1973).
8. H.J. McSkimin and P. Andreatch, Jr., J. Appl. Phys., **35**, 2161 (1964).